EXPERIMENTAL STUDIES OF ELECTRON AND GAS SOURCES IN A HEAVY-ION BEAM*

A. W. Molvik#, R. H. Cohen, A. Friedman, M. Kireeff Covo , S. M. Lund, Lawrence Livermore National Laboratory, Heavy Ion Fusion Virtual National Laboratory, Livermore, CA 94550, USA.
P. A. Seidl, F. M. Bieniosek, A. Faltens, L. Prost, Lawrence Berkeley National Laboratory, Heavy Ion Fusion Virtual National Laboratory, Berkeley CA 9472-82010, USA

Abstract

We use the High Current Experiment (HCX) to study three mitigation measures: a rough surface to reduce electron emission and gas desorption from ions striking walls near grazing incidence, a suppressor electrode after the magnets to block beam-induced electrons off the end structures from drifting upstream, and clearing electrodes to remove electrons from drift regions between magnets. We find that each technique performs as intended.

INTRODUCTION

Electron cloud effects (ECEs) [1] and beam-induced pressure rises [2], that are frequently observed to limit the performance of colliders and high-intensity rings, are also a concern for future high-intensity heavy ion linear accelerators such as envisioned in Heavy Ion Inertial Fusion (HIF) [3]. Electron clouds have thus far been a problem only in rings where the beam passes the same location many times. However, HIF linacs have characteristics that may cause ECEs to be a concern: (1) The cost of accelerators for HIF can be reduced by fitting beam tubes more tightly to beams. This places them at risk from gas desorption runaway, and from electron clouds produced by secondary electrons and ionization of gas. (2) Beam space-charge potentials exceed 1 kV, more than sufficient to electrostatically trap electrons. (3) Beam flat-top durations in our conceptual power-plant drivers range from ~30 μs near injection to 0.2 μs at high energies; the longer durations are sufficient for desorbed gas to reach the beam. (4) Electrons emitted from an end wall of a linac that is bombarded by ions can backstream along the beam.

We are engaged in an experimental and theoretical program to measure, understand, and model these effects in heavy-ion accelerators [4,5]. We have found that 1 MeV K^+ ions, incident on a surface near grazing incidence, generate the order of 10^2 electrons (extrapolating as $6/\cos\theta$ to about 6 at normal incidence) and 10^4 gas molecules [6]. The beam will also generate electrons where it dumps on a metal end wall. In this paper, we discuss the use of a suppressor electrode to switch, or control, the flow of electrons from the end wall, measuring the electron flow with clearing electrodes, intended to remove electrons from the drift regions between quadrupole magnets, and using an electrode that lines the beam tube in the last quadrupole magnet as a diagnostic.

On HCX we are using a 1 MeV, 180 mA, K^+ ion beam to study transport [7], beam induced electron emission and gas desorption [6], and electron cloud and gas effects in magnetic quadrupoles [4]. The beam has a space-charge potential of ~2 kV, rise and fall times of 1 μs, and a flattop duration of 4 μs, repeated at 10 s intervals. An aperture can be inserted at the D2 diagnostic region, immediately preceding the magnetic quadrupoles, to reduce the beam current to 25 mA and ~300 V beam potential. Electron transit times between walls are in the range of 4 ns (11 ns if apertured) for an unneutralized beam, almost 3 orders of magnitude shorter than the flattop duration. This enables exploration of unique electron trapping regimes: beam-induced multipactor trapping, that is frequently observed with in rf accelerators, will not occur during the flattop, and trailing edge multipactor is not an issue because any electrons generated will be lost before the next pulse in ~10 s. However electrons, emitted from a beam-tube wall under beam bombardment, will be trapped during the current rise at the beam head. Electrons from an end wall will be pulled into the positive beam potential, and can be transported upstream in quadrupole magnets by electron drifts. Ionization of gas by the beam generates electrons that are deeply trapped; the associated ions from gas are expelled in $\leq$1 μs.

MITIGATION OF EMISSION

Heavy-ion beams impinging on surfaces near grazing incidence (to simulate the loss of halo ions) generate copious amounts of electrons and gas that can degrade the beam. Electron emission and gas desorption coefficients η_e and η_0 respectively, due to ion bombardment of metal surfaces near grazing incidence, have been measured with the Gas-Electron Source Diagnostic (GESD) [6]. The electron emission coefficient, η_e, is measured from the ratio of the emission current off a target electrode to the beam current into the GESD that is measured with a Faraday cup. The gas desorption coefficient, η_0, is measured from the pressure rise after a pulse compared with the time-integral of the beam current into the GESD Faraday cup. The GESD pumps out through the 0.3 by 2.5 cm entrance aperture, plus a 1 cm diameter hole, giving a pump-out time constant of 0.3 s, long enough for an ion gauge to determine the peak pressure, but short compared with the 10 s before the next pulse.

* Work supported by US DOE contracts W-7405-Eng-48 and DE-AC03-76F00098.
# molvik1@llnl.gov

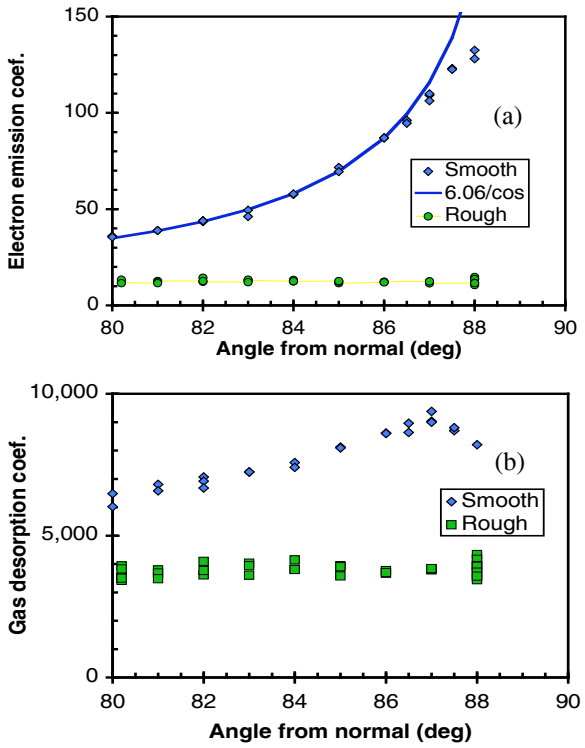

Fig. 1. (a) Electron emission coefficient as a function of angle of incidence, measured from normal to the stainless steel target. [blue-diamonds] Data from a smooth target. The blue line, given by 6.06/cosθ, is a fit to the data between 80° and 86°. [Green circles] Data from a surface roughened by bead blasting. (b) [blue diamonds] Gas desorption coefficient data from a smooth surface; [green squares] similar data from a bead-blasted surface.

This information enables us to interpret electron emission currents from electrodes in beam tubes in terms of the beam-halo loss that caused the emission, and to infer the resulting gas desorption. The GESD is also useful for studying mitigation techniques. We find that $\eta_e \sim 10^2$ and $\eta_0 \sim 10^4$ for 1 MeV K^+ ions incident on smooth stainless steel [6]. The dependence of the electron emission coefficient η_e on the ion angle of incidence is observed to scale as $\eta_e \propto d/\cos\theta$, where $d/\cos\theta$ is the ion path length through a thin $d \approx 2$ nm thick surface layer (where the beam-induced electrons originate). Similar scaling was previously observed at higher ion energies by Thieberger [8]. The angular dependence of gas desorption is much less than $1/\cos\theta$. Similar gas desorption scaling with angle of incidence is observed at higher ion energies by Mahner [9].

One mitigation technique takes advantage of electron emission scaling as $\eta_e \propto 1/\cos\theta$, where θ is the ion angle of incidence relative to normal. If we were to roughen a surface by blasting it with glass beads, then ions that were near grazing incidence (90°) on smooth surface would strike the rims of the micro-craters at angles closer to normal incidence. This should reduce electron emission: the factor of 10 reduction that we observed, Fig. 1(a), implies an average angle of incidence of 62°. Gas desorption varies more slowly with θ (Fig. 1(b)) decreasing a factor of ~2, and along with the electron emission is independent of the angle of incidence on a rough surface.

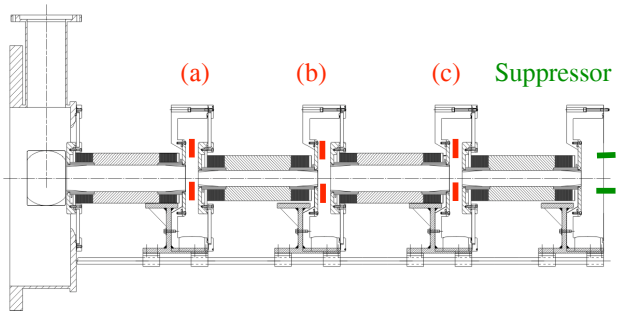

Fig. 2. Magnetic quadrupole region of HCX, from D2 diagnostic region on the left to the D-End diagnostic region beginning on the right. Clearing electrodes a, b, and c are shown in the drift regions between each pair of quadrupoles. A suppressor electrode prevents beam induced electron emission, from structures hit by beam in D-End, from reaching the quadrupole magnets.

SUPPRESSOR AND CLEARING ELECTRODES

The HCX in the region of four magnetic quadrupoles is shown in Fig. 2. To the left is the D2 diagnostic region between 10 electrostatic quadrupoles and the 4 magnetic quadrupoles. Each magnetic quadrupole has 30 cm long magnetic field coils in a 47 cm long elliptical tube that has minor and major inner radii of 3 cm and 5 cm respectively. The half-lattice length is 0.52 m. Between each pair of magnets, and after the last one, diagnostic access is provided in a 5 cm gap, each with 7 ports.

Clearing electrodes were installed in the 5 cm gaps between quadrupole magnets for the purpose of sweeping electrons from each drift region by applying a positive bias voltage. Each clearing electrode is a ring with an inner diameter of 8 cm and a minor diameter of 1.3 cm, which places the electrodes about 1 cm outside of the magnet bore such that beam halo ions do not strike the electrodes, Fig. 2. A capacitive electrode, 28 cm long, surrounding the beam and nearly flush to the 3 x 5 cm radius magnet bore was installed in the fourth magnetic quadrupole. A suppressor ring, that is 10 cm diameter and 10 cm long, was installed surrounding the beam after it exits the last magnet. It can be biased to –10 kV to prevent electrons that are created by beam impinging on metal surfaces from being transported back into the quadrupole magnets. For these experiments, the front plate of a slit scanner is inserted, providing a grounded metal surface on which the ion beam impinges, generating ≥6 electrons per incident ion [6]. It is located about 30 cm from where the field of the last quadrupole magnet ends.

Downstream of the last quadrupole magnet, the 1 MeV beam, with v_b = 2.3 m/μs, strikes a grounded metal slit plate at a distance of 0.33 m, emitting an electron current

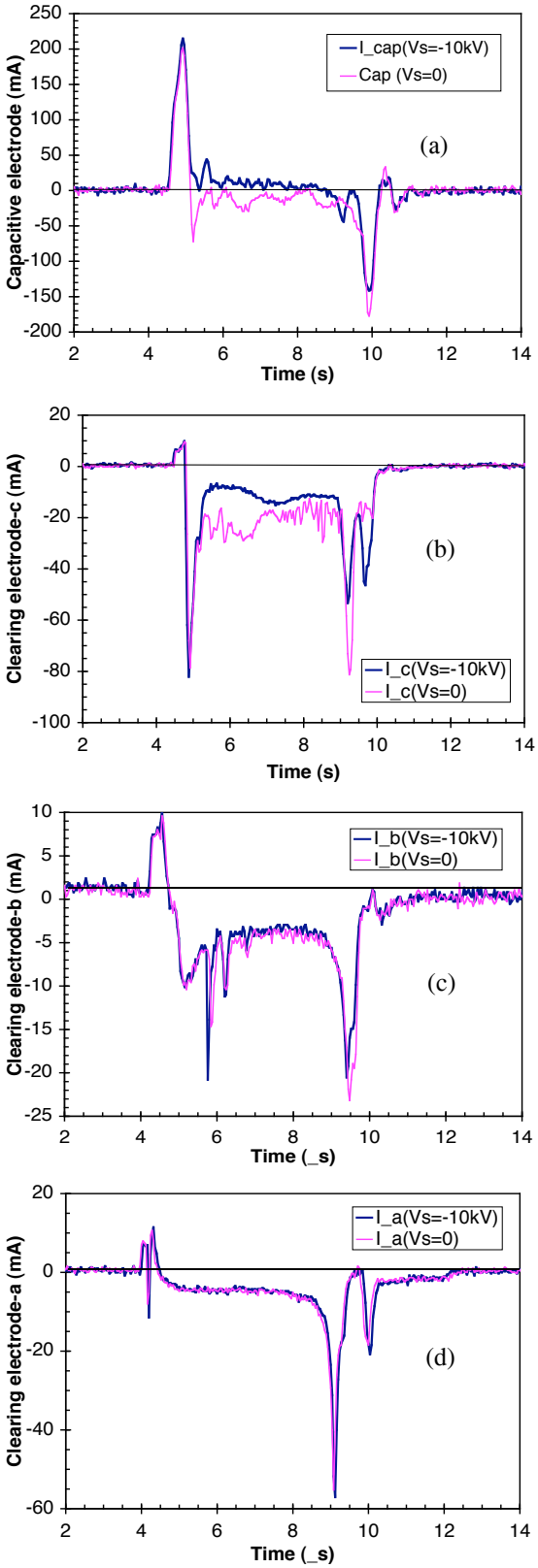

Fig. 3. Currents to (a) a capacitive electrode in magnet 4, (b) clearing electrode c between magnets 3 and 4, (c) clearing electrode b between magnets 2 and 3, and (d) clearing electrode a between magnets 1 and 2 (See Fig. 2 for locations).

of at least 6 times the beam current. When the suppressor electrode is off, electrons can fill the beam in the drift region to $n_e \sim n_b$ in a time

$$\tau = \frac{0.33\ \text{m}}{6 \times 2.3\ \text{m}/\mu\text{s}} = 0.024\ \mu\text{s}$$

The currents to a capacitive electrode in the fourth magnet and to each of three clearing electrode are shown in Fig. 3 with the suppressor electrode biased to 0 and –10 kV. The capacitive electrode shows the expected positive value during the beam head and negative value during the tail, Fig. 3(a). During the nearly flat portion of the beam pulse, the capacitive current is positive with the suppressor biased to –10 kV, consistent with electron emission from the electrode into the positive beam potential. For a suppressor bias of 0 kV, the current to the capacitive electrode is mostly negative, indicating that more electrons are flowing into the electrode than are being emitted. These measurements are consistent with the suppressor functioning as intended: when biased to –10 kV, it prevents electrons generated downstream from reaching the quadrupole magnets, therefore fewer electrons are available to flow into the capacitive electrode, and the beam potential enhances the flow of electrons that are emitted from the capacitive electrode when struck by beam halo ions.

The current to clearing electrode c (between the third and fourth quadrupole magnets) is also strongly affected by the suppressor electrode, decreasing by about a factor of two when the suppressor is on at –10 kV, Fig. 3(b). This demonstrates that electrons drift upstream through the fourth quadrupole magnet to reach clearing electrode c. However, the currents to clearing electrodes a and b are unaffected by the suppressor bias, the currents are nearly identical to electrode b and even more identical to electrode a, Fig. 3(c,d). To better quantify how similar the currents are, we average the difference in the currents between 7 and 8.5 μs, finding that the change in current to electrode a is 0.2±0.6 mA, while that to electrode b is 0.6±0.6 mA, both small compared with the change in current to clearing electrode c current of ~5-20 mA. This demonstrates that clearing electrode c is performing as it was intended to; it removes essentially all electrons from the drift region between magnets 3 and 4.

ACKNOWLEDGEMENTS

We are grateful to Ralph Hipple, William Strelo, Tak Katayanagi, Gary Ritchie, Craig Rogers, and Ed Romero for excellent technical support.

REFERENCES

[1] http://wwwslap.cern.ch/collective/ecloud02/proceedings/index.html

[2] S. Y. Zhang, "ICFA Workshop on Beam Induced Pressure Rise in Rings," http://www.c-ad.bnl.gov/icfa (2003).

[3] R. O. Bangerter, Phil. Trans. R. Soc. Lond. A **357**, 575 (1999).

[4] A. W. Molvik, R. Cohen, A. Friedman, S. Lund, et al., "Initial Experimental Studies of Electron Accumulation in a Heavy-Ion Beam," Proc. 2003 Particle Accelerator Conference, p. 312 (IEEE, 2003).

[5] R. H. Cohen, A. Friedman, S. M. Lund, A. W. Molvik, M. Furman, J.-L. Vay, and P. Stoltz, Proc. 2003 Particle Accelerator Conference, p. 132 (IEEE, 2003).
[6] A. W. Molvik, M. Kireeff Covo, F. M. Bieniosek, L. Prost, P. A. Seidl, D. Baca, A. Coorey, and A. Sakumi, "Gas desorption and electron emission for 1 MeV potassium ion bombardment of stainless steel," to be published in PRST-AB (2004).
[7] L. Prost, "The High-Current transport Experiment for heavy-ion inertial fusion", submitted to PRST-AB.
[8] P. Thieberger, A. L. Hanson, D. B. Steski, S. Y.Z. V. Zajic, and H.Ludewig, Phys. Rev. A. **61**, 042901 (2000).
[9] E. Mahner, J. Hansen, J.-M. Laurent, and N. Madsen, PRST-AB **6**, 013201 (2003).
[10] J. F. Ziegler, http://www.srim.org/.
[11] R. H. Cohen, et al., HIF-04.